

Insight on Hole-Hole Interaction and Magnetic Order from Dichroic Auger-Photoelectron Coincidence Spectra

M. Cini,^{1,2} E. Perfetto,¹ R. Gotter,³ G. Offi,⁴ A. Ruocco,⁴ and G. Stefani⁴

¹*Dipartimento di Fisica, Università di Roma Tor Vergata,
Via della Ricerca Scientifica 1, I-00133 Rome, Italy*

²*Laboratori Nazionali di Frascati, Istituto Nazionale di Fisica Nucleare, Via E. Fermi 40, 00044 Frascati, Italy*

³*IOM-CNR Istituto Officina dei Materiali del CNR, Area Science Park - Basovizza, Trieste, Italy*

⁴*CNISM and Dipartimento di Fisica, Università di Roma Tre-Rome, Italy*

The absence of sharp structures in the core-valence-valence Auger line shapes of partially filled bands has severely limited the use of electron spectroscopy in magnetic crystals and other correlated materials. Here by a novel interplay of experimental and theoretical techniques we achieve a combined understanding of the Photoelectron, Auger and Auger-Photoelectron Coincidence Spectra (APECS) of CoO. This is a prototype antiferromagnetic material in which the recently discovered Dichroic Effect in Angle Resolved (DEAR) APECS reveals a complex pattern in the strongly correlated Auger line shape. A calculation of the *unrelaxed* spectral features explains the pattern in detail, labeling the final states by the total spin. The present theoretical analysis shows that the dichroic effect arises from a spin-dependence of the angular distribution of the photoelectron-Auger electron pair detected in coincidence, and from the selective power of the dichroic technique in assigning different weights to the various spin components. Since the spin-dependence of the angular distribution exists in the antiferromagnetic state but vanishes at the Néel temperature, the DEAR-APECS technique detects the phase transition from its local effects, thus providing a unique tool to observe and understand magnetic correlations in such circumstances, where the usual methods (neutron diffraction, specific heat measurements) are not applicable.

PACS numbers: 82.80 Pv, 79.60-i, 75.70.Rf

The Auger Core-Valence-Valence (CVV) transitions, that produce a pair of holes in the valence states of an atom in a solid, have long been of interest. Powell[1] pointed out that some crystals have broad band-like CVV profiles while others show atomic-like multiplet spectra. In the Cini-Sawatzky theory[2–4], which, with some refinements, yields accurate line shapes[5] without free parameters[6], the line shape gives details of the on-site dynamics and screened interactions in solids. Strong correlations produce two-hole resonances and atomic-like spectra, while weak correlations produce a distortion of the band self-convolution. The short range of the Auger matrix elements (a few atomic units) ensures that the information is *local* (that is, available also from tiny inhomogeneous samples) and microscopic in character. Early work was limited to closed (i.e. fully occupied) valence bands. An extension[7] to open bands with an occupation of at least $\sim 90\%$ led to the Bare-Ladder Approximation[8–10]. This theory provides accurate results for photoemission and Auger spectra in cases like Pd metal[10]. However at lower filling the open bands polarize strongly around the primary core hole. Then, the dynamics is more involved since it cannot be described in terms of the propagation of two holes, and the theoretical analysis complicates substantially[11–16]. In a simplified approach proposed by Drchal and one of us[12], some spectral features are *unrelaxed*, i.e., arise from the propagation of two holes in a unpolarized rigid background, similar to the closed-bands case; the *relaxed* part of the spectrum comes instead from a screened situation and

involves the screening cloud. Anyhow for decades, little information has been gained from open-band spectra. Indeed, the Auger $L_{23}VV$ line shape from metals like Cr, Fe, Co and compounds like CoO are almost featureless[17], characterized by broad structures, eventually with little Coster-Kronig satellites[18]. However, despite the spectra have a band-like look, the magnetic properties of these solids indicate that correlations must be quite strong.

The APECS (Auger-Photoelectron Coincidence Spectroscopy) technique measures Auger spectra originated by a specific core-hole state. Important input came from the further discovery[19–21] that the coincidence Auger electron energy distribution depends on the emission angle of both Auger electron and Photoelectron. This was called Dichroic Effect or DEAR APECS. It was argued that spin-symmetric (i.e., high-spin) and spin-antisymmetric (i.e., low-spin) final states are enhanced or suppressed depending upon the chosen geometry, but this lacked theoretical support.

In this Letter we show that substantial progress in the understanding of magnetic correlations in open bands solids can be achieved by the interplay between theory and the DEAR-APECS technique. We model the CoO crystal by an octahedral CoO_6 cluster centered on the Co ion. We include a minimal basis set and fix the parameters of the model by comparing the calculated Local Density of States (LDOS) with the experimental XPS profile. Then, we show how it is possible to reveal considerable structure in the Auger data, and interpret it in

terms of the spin selectivity of APECS. Finally we point out that this case study has general implications about electron spectroscopy and also in the field of magnetism.

The linear combinations of $3d$ orbitals which form the e_g and t_{2g} irreducible representations (irreps) of the Octahedral Group are a suitable one electron basis for the Co ion. We take into account only the combinations of $2p$ orbitals with symmetry e_g and t_{2g}

$$p_{\Gamma\gamma} = \sum_{j=x,y,z} c_{Jj}^{\Gamma\gamma} p_{Jj}, \quad (1)$$

where J runs over the 6 Oxygens, Γ runs over the irreps and γ over the corresponding components. In this basis the non-interacting part of the Hamiltonian reads

$$H_0 = \sum_{\Gamma=e_g,t_{2g}} \sum_{\gamma} \left[\epsilon_d(\Gamma) d_{\Gamma\gamma}^\dagger d_{\Gamma\gamma} + \epsilon_p(\Gamma) p_{\Gamma\gamma}^\dagger p_{\Gamma\gamma} + t_{pd}(\Gamma, \gamma) (d_{\Gamma\gamma}^\dagger p_{\Gamma\gamma} + p_{\Gamma\gamma}^\dagger d_{\Gamma\gamma}) \right] \quad (2)$$

where we take $\epsilon_d(e_g) = \Delta - 6D$, $\epsilon_p(e_g) = -(\epsilon_\sigma - \epsilon_\pi)$ and $\epsilon_d(t_{2g}) = \Delta + 4D$, $\epsilon_p(t_{2g}) = \epsilon_\sigma - \epsilon_\pi$. The hopping parameters are the following linear combinations of Slater-Koster matrix elements [22] $E_{\Gamma\gamma,j}(J)$:

$$t_{pd}(\Gamma, \gamma) = \sum_{j=x,y,z} c_{Jj}^{\Gamma\gamma} E_{\Gamma\gamma,j}(J). \quad (3)$$

In the above Equation the Oxygen J is specified by the direction cosines (l, m, n) and the energies $E_{\Gamma\gamma,j}(J)$ are expressed in terms of τ_σ and τ_π transfer integrals. As in previous works[2, 3] we include the on-site repulsion in the Co ion and neglect it on the O sites. The interaction part of the Hamiltonian is taken in the standard form:

$$H_{\text{int}} = \sum_{mm'nn'} \sum_{\sigma\sigma'} U_{mm'nn'} d_{m\sigma}^\dagger d_{m'\sigma'}^\dagger d_{n'\sigma'} d_{n\sigma}, \quad (4)$$

where the m, m', n, n' run over the Co orbitals; the $U_{mm'nn'}$ elements can be written in terms of Slater integrals which, in turn, are expressed in terms of the Racah parameters[23] A, B, C according to $f^4 = \frac{63}{5}C$, $f^0 = A + \frac{1}{9}f^4$, $f^2 = \frac{441}{9}B + \frac{5}{9}f^4$. As only A is affected by the solid state screening we use $B = 0.14$ eV and $C = 0.54$ eV like in the isolated Co[23]. Eventually by a unitary transformation we rewrite H_{int} in the symmetry adapted basis (Γ, γ) .

In the left panel of Fig. 1 we reproduce from Ref. 24 the XPS spectrum obtained by an unmonochromated Mg $K\alpha$ line. Using the above geometry and basis set, van Elp and coworkers also computed the Co LDOS[24] by a continued fraction technique (excluding some higher energy configurations) with a Lorentzian broadening of 1 eV. The 3-holes ground state (d^7 configuration) was taken to belong to maximum spin $S = 3/2$ in agreement with Hund's rule. Choosing the parameters that gave a

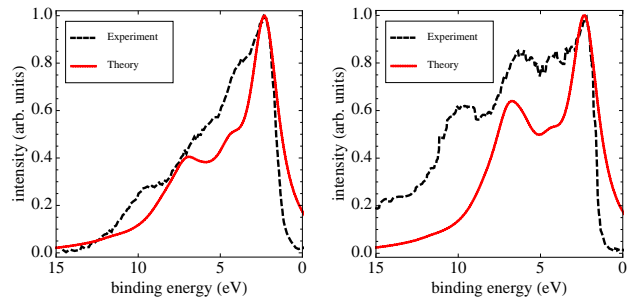


FIG. 1. Comparison of experimental and calculated valence-band XPS profiles. Left panel: the spectrum excited by 1253.6 eV X-rays from Ref. 24 (dashed line) and our calculated Co-removal spectrum (solid line). Right panel: the spectrum excited by 250 eV X-rays from Ref. 25 (dashed line) and our calculated (0.8Co + 0.2O)-removal spectrum (solid line). In the calculated spectra a 1 eV Lorentzian broadening was used.

visual agreement with their XPS spectrum, they estimated $A = 5.2$ eV. In the right panel of Fig. 1 we also report the profile obtained by soft X-Rays from Ref. 25. The lower energy of the incident photons gives rise to a rather different spectrum. The difference can be understood qualitatively because the ionization cross section for p states drops with frequency faster than that of the more localized d states, and so soft X-Rays data have much stronger oxygen character.

The exact diagonalization of CoO₆ model Hamiltonian with 3 holes shows that the ground state with the parameters of Ref. 24 is at energy -11.78 eV for spin 3/2 and -13.03 eV for spin 1/2. Thus Hund's rule does *not* apply unless A is considerably increased with the consequence, however, of deteriorating the agreement with experimental profile. We interpret this result as an artifact of the small cluster, which reduces the degeneracy of one-electron levels forcing the electrons to arrange in a low-spin configuration. Therefore, we consider the $S = 3/2$ sector as the most appropriate one for modeling the actual solid. Taking (in eV) $\Delta = 5.5$, $D = 0.07$, $\epsilon_\sigma = 0.55$ and $\epsilon_\pi = -0.15$ as in Ref.24 we diagonalised the Hamiltonian with 4 holes and computed the LDOS at the Co and O sites, looking for the best Racah A . The priority for the theory is to reproduce the positions of the most prominent features at lower binding energies, which are similar in both spectra. To ensure that the prominent narrow peak near the Fermi level has a dominant Co character in both cases, and correctly produce the enhancement of the structure (with dominant O character) at 7.4 eV in the right panel, we need $A = 1.08$, which is definitely smaller than the value found in Ref. [24]. In Fig. 1 we display the pure Co profile (left panel, solid curve) and, according to the above discussion, the one with 20% Oxygen component (right panel, solid curve).

To conclude the part on XPS we stress that the spec-

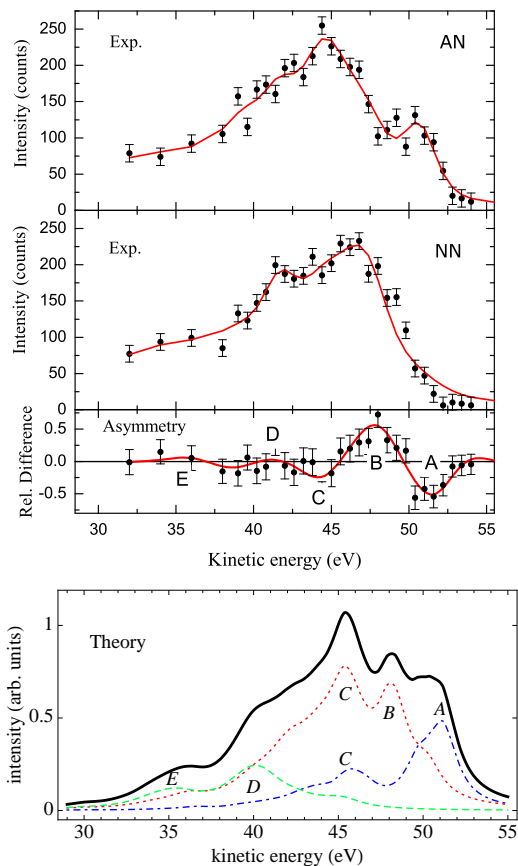


FIG. 2. (Color online) Top panel: Experimental DEAR-APECS spectra of CoO *vs* Auger electron kinetic energy for the AN and NN geometry, and their difference (dashed). The continuous AN and NN lines are obtained by a best fit procedures based on a representation of the experimental line shapes by six Voigt profiles (see main text). The difference (or asymmetry curve) displays structures labeled by A – E. Bottom panel: Calculated total Auger spectrum (solid line) and the different contributions corresponding to the spin $S = 5/2$ (dot-dashed) $S = 3/2$ (dotted) $S = 1/2$ (dashed) of the final state. The structures A – E are reproduced by the theory. In addition, C has a shoulder at ~ 43 eV which is not evident in the asymmetry curve because it appears in both the $S = 5/2$ and $S = 3/2$ spectra, but is clearly seen in both the AN and NN data.

trum does not change significantly as the temperature is increased from $T = 170$ K (in the AF phase) to $T = 295$ K (above the Néel temperature).

The experimental $M_{23}M_{45}M_{45}$ Auger spectra of CoO from Ref. 25 (and reported in the upper panels of Fig. 2) were measured in coincidence with the photoelectron current excited from the Co $3p_{3/2}$ core level. The profiles marked AN and NN are APECS spectra taken at different angles, at a low temperature, i.e., with the CoO film in the AF phase. The notation NN means that both electrons are not aligned (N) with the photon polarization whereas AN means that the photoelectron is aligned with the photon polarization while the Auger electron is

Feature	A	B	C	D	E
Spin	5/2	3/2	3/2, 5/2	1/2	1/2
Theory (eV)	51.5	48.0	45.4	40.3	35.5
Experiment (eV)	50.7	47.2	44.6	39.5	34.7
Intensity AN	285	377	1020	301	361
Intensity NN	64	785	819	308	365

TABLE I. Main features in the APECS spectrum of CoO, characterized by their kinetic energies, relative intensities and main spin components. The experimental energies and intensities are obtained by the best fit described in the text.

not. It was observed[25] that the low-spin two-hole final states are favored in the NN geometry while the AN configuration favors high-spin (DEAR APECS effect). By comparing AN and NN spectra, a clear modulation of the line shape is obtained and sharp peaks emerge. In particular the asymmetry curve (i.e., the difference between NN and AN spectra) displays a fingerprint, which cannot be seen in the *singles* spectrum. The most remarkable point is that effect is lost above the Néel temperature[25] while XPS and the singles Auger lines do not change at the transition.

We below address this issue and calculate the Auger the unrelaxed spectrum[12] without any adjustable parameter, keeping the values optimized for the XPS line-shape. The M_{45} final-state holes belong to the Co $3d$ -O $2p$ valence band. Up to a proportionality constant, the Auger current $J(\epsilon_k)$ with wavevector k after the absorption of a photon of energy ω by a core level c , and accompanied by a photoelectron of energy ϵ_p is

$$J(\epsilon_k) = \sum_{\alpha, \beta, \gamma, \delta} M_{ck\alpha\beta}^* M_{ck\gamma\delta} D_{\alpha\beta\delta\gamma}(\epsilon_p + \epsilon_k - \omega), \quad (5)$$

where $-\pi D_{\alpha\beta\delta\gamma}(\omega)$ is the imaginary part of the Fourier transform of the retarded the Green's function

$$G_{\alpha\beta\gamma\delta}(t) = -\langle T [d_{\beta}^{\dagger}(t) d_{\alpha}^{\dagger}(t) d_{\gamma} d_{\delta}] \rangle, \quad (6)$$

and $M_{ck\alpha\beta}$ is the Auger matrix element, obtained by the Coulomb integral between the core state c , the Auger electron k , and the two valence states labelled by α and β . We computed the $M_{ck\alpha\beta}$ matrix elements for the $M_{23}M_{45}M_{45}$ transitions using the Clementi-Roetti atomic orbitals [26] for positive ions and plane-waves for the Auger electrons; only the diagonal contributions $(\alpha, \beta) = (\gamma, \delta)$ in Eq. (5) were included and the direction of the momentum k was taken along the quantization axis of the Co ion. Such a simple treatment is reasonable since we are not aiming at absolute rate calculations but at computing the line shape. A Lorentzian of width 1 eV was convolved to the function J to simulate lifetime and any other broadening effects.

The CoO₆ cluster (10 orbitals) hosts 5 holes after the Auger decay and the rank of the problem is $\binom{20}{5} = 15504$. Let H_{nm} denote the Hamiltonians with m spin-up and n spin-down holes; we put H_{50}, H_{41} and H_{32} in block form using the total spin S symmetry and found the eigenvectors of the blocks. H_{32} has 252 sextets, 1848 quartets and 3300 doublets which form the biggest block. In the bottom panel of Fig. 2 we report the calculated, spin-resolved Auger spectrum. The dot-dashed, dotted and dashed lines show the contribution of $S = 5/2$, $S = 3/2$ and $S = 1/2$ respectively, while the solid line is the total angular unresolved spectrum. The letters $A - E$ are used to mark the main features whose maxima in energy are reported in Table I.

To make comparison of theory and experiment, we need to know the positions of the experimental peaks. To this end, we represented the AN and NN spectra by superpositions of six Voigt profiles and made partial best fits. The results are shown in Table I. Taking into account that in the experiment of Ref. 25 no absolute calibration of the Auger energy scale was performed and that an overall uncertainty of ± 0.4 eV is estimated, the energy position of the five main structures correspond very well with the theoretical predictions for both geometries.

The present theoretical analysis demonstrates that the DEAR-APECS technique detects structure in the line shape because the AN and NN geometries discriminate the spin components; A which is mainly $S = 5/2$ prevails in AN while B which is mainly $S = 3/2$ weights more in NN. Qualitatively, the different spin contents of structures A and B had been conjectured already in Ref. 25 based on a Tanabe-Sugano [27] analysis of the data. The present more quantitative work validates this picture and shows that the same occurs at lower kinetic energies too (features D and E) where a similar dichroism occurs between $S = 1/2$ and $S = 3/2$. The best fit intensities reported in Tab. I show that the NN geometry generally favors high spin states of the final ion and the AN geometry prefers low spin; in general terms, the APECS geometry strongly affects the probability of leaving the Co ion in different spin states.

Equation (5) can capture only the *unrelaxed* spectrum and is already sufficient to assign the main structures. The *relaxed* spectrum must be responsible for the broad and rather flat background that one sees in the experimental profile, but *a posteriori* we conclude that it does not play a very important role in this case. This may be due to a short $3p$ lifetime (the energy width of the $3p$ photoemission line is found to be 1.1 eV) or to slow screening of the core-hole.

In conclusion, by a tight interplay of theory and experiment we succeeded to observe, identify and characterize in some detail the final states of a core-valence-valence transition in a correlated open band. This finding solves a long standing problem and is an important achieve-

ment in the field of electron spectroscopy. Previously, such spectra had been misinterpreted as band-like despite the fact that the materials had magnetic properties. The spin selectivity is inherent in the dichroic technique, since the ion spin governs the angular distribution of the photoelectron-Auger electron pair, thus allowing to monitor the magnetism at the ion site. We must tackle new exciting problems, including a full theory of the operation of DEAR-APECS. An extended theory should explain the disappearance of the effect in the paramagnetic phase, that is, why not only S_z but also S fluctuates during the lifetime of the core-hole fast enough to kill the effect. In this way, we will be able to better understand and exploit its implications as a local probe of the magnetic order in solids.

ACKNOWLEDGMENT

Financial support from the MIUR PRIN 2008 contract prot. 2008AKZSXY is gratefully acknowledged.

-
- [1] C. J. Powell, Phys. Rev. Lett. **30**, 1179 (1973).
 - [2] M. Cini, Solid State Commun. **20**, 605 (1976).
 - [3] M. Cini, Solid State Commun. **24**, 681 (1977).
 - [4] G. A. Sawatzky, Phys. Rev. Letters **39**, 504 (1977).
 - [5] P. Weightman, Rep. Prog. Phys. **45**, 752, (1982); R. J. Cole, C. Verdozzi, M. Cini, P. Weightman, Phys. Rev. **B** **49** (1994) 13329.
 - [6] G. Fratesi, M.I. Trioni, G.P. Brivio, S. Ugenti, E. Perfetto, and M. Cini, Phys. Rev. **B** **78**, 205111 (2008)
 - [7] M. Cini, Surface Sci. **87**, 483 (1979).
 - [8] V. Galitzkii, Soviet Phys. JETP **7**, 104 (1958).
 - [9] M. Cini and C. Verdozzi, J. Phys. C **12**, 7457 (1989).
 - [10] M. Cini, M. De Crescenzi, F. Patella, N. Motta, M. Sastry, F. Rochet, R. Pasquali, A. Balzarotti, C. Verdozzi, Phys. Rev. **B** **41** 5685 (1990).
 - [11] O. Gunnarsson and K. Schönhammer, Phys. Rev. **B** **26**, 2765 (1982).
 - [12] M. Cini and V. Drchal, Journal of Electron Spectroscopy and Rel. Phen. **72**, 151 (1995).
 - [13] A. Marini and M. Cini, Journal of Electron Spectroscopy and Rel. Phen. **127**, 17 (2002).
 - [14] S. Ugenti, M. Cini, G. Seibold, J. Lorenzana, E. Perfetto, and G. Stefanucci, Phys. Rev. **B** **82** 075137, (2010).
 - [15] E. Perfetto, Phys. Rev. **B** **77**, 115401 (2008).
 - [16] E. Perfetto, M. Cini, S. Ugenti, P. Castrucci, M. Scarselli, M. De Crescenzi, F. Rosei, and M. A. El Khakani, Phys. Rev. **B** **76**, 233408 (2007).
 - [17] C. P. Lund, S. M. Thurgate and A. B. Wedding, Phys. Rev. **B** **55**, 5455 (1997).
 - [18] Michele Cini, Enrico Perfetto, Gianluca Stefanucci and Simona Ugenti, Phys. Rev. **B** **76**, 205412 (2007)
 - [19] H. Haak, G. A. Sawatzky and T. D. Thomas, Phys. Rev. Lett. **41**, 1825 (1978).
 - [20] G. Stefani, R. Gotter, A. Ruocco, F. Offi, F. Da Pieve, S. Iacobucci, A. Morgante, A. Verdini, A. Liscio, H. Yao,

- R.A. Bartynski, *Journal of Electron Spectroscopy and Rel. Phen.* **141**, 149 (2004).
- [21] R. Gotter, F. Da Pieve, A. Ruocco, F. Offi, G. Stefani and R.A. Bartynski, *Phys. Rev. B* **72** 235409 (2005); R. Gotter, F. Da Pieve, F. Offi, A. Ruocco, A. Verdini, H. Yao, R.A. Bartynski and G. Stefani, *Phys. Rev. B* **79**, 075108 (2009).
- [22] J. C. Slater and G. F. Koster, *Phys. Rev.* **94**, 1498 (1954).
- [23] G. Racah, *Phys. Rev.* **62** 438 (1942).
- [24] J. van Elp, J.L. Wieland, H. Eskes, P. Kuiper, and G.A. Sawatzky, *Phys. Rev. B* **12**, 6090 (1991).
- [25] R. Gotter, F. Offi, A. Ruocco, F. Da Pieve, R. Bartynski, M. Cini and G. Stefani, *Europhys. Lett.* **94**, 37008 (2011).
- [26] E. Clementi and C. Roetti, *ATOMIC DATA AND NUCLEAR DATA TABLES* **14**, 177-478 (1974).
- [27] Y. Tanabe and S. Sugano, *J. of Phys. Soc. of Japan* **11**, 864 (1956).